



**HAL**  
open science

## Corrosion Products Electrochemical Behaviour into Molten LiF-NaF: Investigation of Cr(II) System

Laurent Massot, Mathieu Gibilaro, D. Quaranta, Pierre Chamelot

► **To cite this version:**

Laurent Massot, Mathieu Gibilaro, D. Quaranta, Pierre Chamelot. Corrosion Products Electrochemical Behaviour into Molten LiF-NaF: Investigation of Cr(II) System. *Journal of The Electrochemical Society*, 2021, 168 (2), pp.026510. 10.1149/1945-7111/abe088 . hal-04142900

**HAL Id: hal-04142900**

**<https://hal.science/hal-04142900>**

Submitted on 5 Jul 2023

**HAL** is a multi-disciplinary open access archive for the deposit and dissemination of scientific research documents, whether they are published or not. The documents may come from teaching and research institutions in France or abroad, or from public or private research centers.

L'archive ouverte pluridisciplinaire **HAL**, est destinée au dépôt et à la diffusion de documents scientifiques de niveau recherche, publiés ou non, émanant des établissements d'enseignement et de recherche français ou étrangers, des laboratoires publics ou privés.



# Corrosion Products Electrochemical Behaviour into Molten LiF-NaF: Investigation of Cr(II) System

L. Massot,<sup>\*,z</sup>  M. Gibilaro, D. Quaranta, and P. Chamelot<sup>\*</sup>

Laboratoire de Génie Chimique; Université de Toulouse; CNRS; INPT; UPS; Toulouse, France

In this work, a detailed electrochemical study of the molten LiF-NaF-CrF<sub>2</sub> system is provided on Ag electrode in the 750 °C–900 °C temperature range. The first part was dedicated to the electrochemical study, by cyclic and square wave voltammetries, allowing the determination of thermodynamic and physico-chemical data such as CrF<sub>2</sub>/Cr standard potential, diffusion coefficient, activity coefficient, transfer energy and nucleation overvoltage. The influence of Li<sub>2</sub>O addition on the electrochemical reduction pathway of dissolved CrF<sub>2</sub> on a silver electrode was investigated. The results showed that an increase of Li<sub>2</sub>O activity in the solution causes CrF<sub>2</sub> disproportionation into solid chromium oxide and metallic Cr.

© 2021 The Author(s). Published on behalf of The Electrochemical Society by IOP Publishing Limited. This is an open access article distributed under the terms of the Creative Commons Attribution 4.0 License (CC BY, <http://creativecommons.org/licenses/by/4.0/>), which permits unrestricted reuse of the work in any medium, provided the original work is properly cited. [DOI: 10.1149/1945-7111/abe088]



Manuscript submitted December 11, 2020; revised manuscript received January 25, 2021. Published February 5, 2021. *This paper is part of the JES Focus Issue on Molten Salts and Ionic Liquids II.*

Nickel-based alloys, composed of many metallic elements such as Cr, Fe, Mo, W, are commonly used in industrial applications involving aggressive conditions due to their corrosion resistance. Beginning with investigations on the Molten Salt Reactor (MSR) in the Oak Ridge National Laboratory (ORNL) in the 1950's, molten salts, and particularly molten fluorides, were envisaged to be used as fuel salt.<sup>1</sup> ORNL demonstrated that, during reactor operation time, the redox potential of the salt, expressed by U(IV)/U(III) ratio has a great influence on the corrosion of container material. The fuel react reacts with chromium and leads to its dissolution from reactor inner material. Molten salts have also been envisaged to be used as a coolant because of their high boiling point and high thermal capacity.<sup>2,3</sup> Several structural materials were tested and the results of these studies showed that Ni-based alloys appeared to be more suitable than iron steels.<sup>4,5</sup>

The corrosion behavior of Nickel-based alloys in molten salts has been identified as a significant issue that determines the life time of the reactor structure materials. Among additive elements, chromium has the lowest oxidation potential and is the first one to be oxidized. In most of high temperature environments, Cr oxidation films are formed, improving their corrosion resistance. However, in molten fluoride salts, these oxidation films are unstable and the oxidation of Cr leads to chromium fluorides as possible corrosion products.

Few studies only investigated the electrochemical behavior of chromium(III) into molten fluorides: Yoko et al.<sup>6</sup> and Smith et al.<sup>7</sup> obtained a Cr(III) diffusion coefficient into FLiNaK around  $6 \times 10^{-7} \text{ cm}^2 \cdot \text{s}^{-1}$  at 650 °C, but the Cr(II) study was not detailed.

This paper investigates the behaviour of CrF<sub>2</sub> in a molten fluoride bath (LiF-NaF at eutectic composition), in the 750 °C–900 °C temperature range, using electrochemical techniques such as cyclic and square wave voltammetries. These techniques allowed the evaluation of CrF<sub>2</sub> stability and determination of data such as CrF<sub>2</sub>/Cr standard potential, diffusion coefficient, activity coefficient, transfer energy and nucleation overvoltage. The presence of oxide impurities can greatly influence the stability of molten bath and structural materials. The last part is so dedicated to the influence of Li<sub>2</sub>O addition on the Cr(II) stability into the bath.

## Experimental

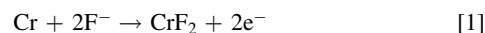
The cell was a vitreous carbon crucible placed in a cylindrical vessel made of refractory steel and closed by a stainless steel lid cooled by circulating water. The inside part of the walls was

protected against fluoride vapours by a graphite liner. The experiments were performed under an inert argon atmosphere (less than one ppm O<sub>2</sub>), previously dehydrated and deoxygenated using a purification cartridge (Air Liquide). The cell was heated using a programmable furnace and the temperatures were measured using a chromel-alumel thermocouple. A more detailed description of the set-up can be found in Ref. 8.

The electrolytic bath consisted of a eutectic LiF-NaF (Merck 99.99%) mixture (60/40 mol%), initially dehydrated by heating under vacuum ( $10^{-5}$  bar) to its melting point (652 °C) for 72 h. Chromium ions were introduced into the bath in the form of CrF<sub>2</sub> powder (VWR 99.99%) and oxide ions in the form of Li<sub>2</sub>O powder (Cerac 99.9%). Silver wire (Goodfellow 99.99%, 1 mm diameter) was used as working electrode. The auxiliary electrode was a vitreous carbon (V25) rod (3 mm diameter) with a large surface area (2.5 cm<sup>2</sup>). The potentials were initially referred to a platinum wire (0.5 mm diameter) immersed in the molten electrolyte, acting as a quasi-reference electrode Pt/PtO<sub>x</sub>/O<sup>2-</sup>. Then, cyclic voltammetry on silver electrode were used in order to determine the equilibrium potential of NaF/Na system. Consequently, all the potentials were thus referred to this equilibrium potential (V vs Na). The electrochemical study, using cyclic voltammetry and square wave voltammetry, and the electrolyses were performed with an Autolab PGSTAT302N potentiostat/galvanostat controlled with NOVA 2.10 software.

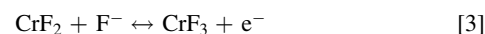
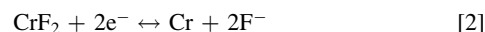
## Results and Discussion

**Preliminary discussion.**—The chromium E-pO<sup>2-</sup> diagram, plotted in Fig. 1 using thermochemical database from HSC 6.1 software at 750 °C (1023 K) with all soluble species activities equal to 0.1 mol kg<sup>-1</sup>, shows that CrF<sub>2</sub> should be the first chromium corrosion product formed by Cr oxidation:



In addition, the electrochemical window is defined by the oxidation of silver and the reduction of NaF, for anodic and cathodic limits respectively.

For low oxide contents, CrF<sub>2</sub> can be reduced into Cr and oxidised into CrF<sub>3</sub> such as:



This observation confirms that the first corrosion product obtained from Cr metal is CrF<sub>2</sub>.

\*Electrochemical Society Member.

<sup>z</sup>E-mail: massot@chimie.ups-tlse.fr

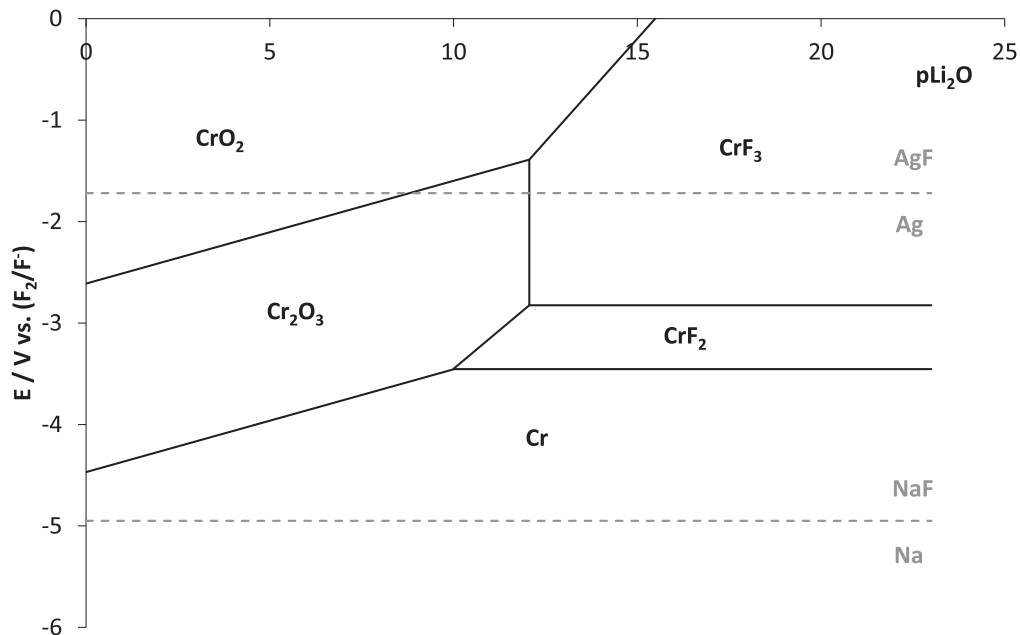
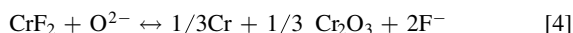


**Figure 1.** Potential-oxoacidity diagram of chromium species in LiF-NaF at 750 °C (1023 K) with all soluble species activities equal to 0.1 mol kg<sup>-1</sup> using thermochemical database from HSC 6.1 software.

– At high O<sup>2-</sup> ions activity ( $pO^{2-} < 12$ ), the disproportionation of CrF<sub>2</sub> into Cr<sub>2</sub>O<sub>3</sub> and Cr is expected as in reaction (4):



This reaction leads to the precipitation of chromium species. To avoid this reaction and thus keep Cr in the form of CrF<sub>2</sub> in the solution, the free oxide content in the bath must be kept at low values.

**Cyclic and square wave voltammetries.**—In this part, the investigation of Cr(II) oxidation and reduction mechanism is described using cyclic and square-wave voltammetries.

**Cyclic voltammetry.**—A typical cyclic voltammogram plotted on a silver electrode in LiF-NaF at 750 °C and 100 mV s<sup>-1</sup>, before (grey line) and after (black line) CrF<sub>2</sub> addition (4.96 10<sup>-2</sup> mol kg<sup>-1</sup>) is presented in Fig. 2a. In agreement with thermodynamic calculations, both electrochemical systems involving CrF<sub>2</sub> oxidation and reduction (CrF<sub>3</sub>/CrF<sub>2</sub> and CrF<sub>2</sub>/Cr) can be observed at around 1.55 and 1.15 V vs Na respectively. The shape of the anodic peak at 1.25 V vs Na is typical of the dissolution of a metal deposited during a cathodic run (stripping peak), in this case Cr. As presented in the Fig. 2b, the reversibility of both systems, characterized by CrF<sub>2</sub> oxidation and reduction peak potentials independent of the scan rate, is verified. Several cyclic voltammograms were plotted for different Cr(II) additions and the obtained value for the slope of the linear relationship between cathodic peak current density and molality is:

$$i_{p(A.cm)}^{-2} = 1.377[CrF_2]_{(mol.kg)}^{-1} \quad [5]$$

Then, the influence of the scan rate on peak intensities for CrF<sub>2</sub> oxidation and reduction was studied (Fig. 2b) to verify the Berzins Delahaye relationship (Eq. 6), valid for a reversible soluble/insoluble system and a diffusion-controlled reaction and Randle-Sevcik one (Eq. 7), valid for a reversible soluble/soluble system and a diffusion-controlled reaction:<sup>9</sup>

$$I_p = -0.61nFSc_0 \left( \frac{nF}{RT} \right)^{1/2} D^{1/2}v^{1/2} \quad [6]$$

$$I_p = 0.446nFSc_0 \left( \frac{nF}{RT} \right)^{1/2} D^{1/2}v^{1/2} \quad [7]$$

where n is the number of exchanged electrons, F the Faraday constant (96500 C mol<sup>-1</sup>), S the electrode surface area in cm<sup>2</sup>, D the diffusion coefficient in cm<sup>2</sup> s<sup>-1</sup>, c<sub>0</sub> the solute concentration in mol cm<sup>-3</sup>, T the absolute temperature in K and v the potential scan rate in V s<sup>-1</sup>.

The slope of these linear equations at 750 °C are:

$$\text{For CrF}_2\text{reduction: } \frac{i_p}{v^{1/2}} = -0.133 \pm 0.002 \text{ A s}^{1/2} \text{ V}^{-1/2} \text{ cm}^{-2} \quad [8]$$

$$\text{For CrF}_2\text{oxidation: } \frac{i_p}{v^{1/2}} = 0.029 \pm 0.002 \text{ A s}^{1/2} \text{ V}^{-1/2} \text{ cm}^{-2} \quad [9]$$

These results prove that both reactions are controlled by CrF<sub>2</sub> diffusion into the solution.

**Square wave voltammetry.**—Square wave voltammetry was carried out in the same previous operating conditions. Typical voltammograms plotted from open-circuit potential (OCP) into anodic and cathodic senses on silver electrode, at 750 °C, 25 Hz, in molten LiF-NaF after CrF<sub>2</sub> addition (4.96 10<sup>-2</sup> mol kg<sup>-1</sup>) are superimposed in Fig. 3.

The following observations can be done from these two SWV:

- Both CrF<sub>3</sub>/CrF<sub>2</sub> and CrF<sub>2</sub>/Cr electrochemical systems are observed in the same potential range than cyclic voltammetry (1.55 and 1.15 V vs Na respectively).
- The sharp decrease of the current observed at the beginning of the CrF<sub>2</sub> reduction peak, associated to the shape of reoxidation peak at 1.15 V vs Na (stripping peak), is typical of metal deposition/reoxidation (Cr) with a nucleation effect.

The inset of Fig. 3 represents the variations of peak potential and peak current density for CrF<sub>2</sub> oxidation and reduction vs the square root of the frequency. Both peak potentials are constant whatever the

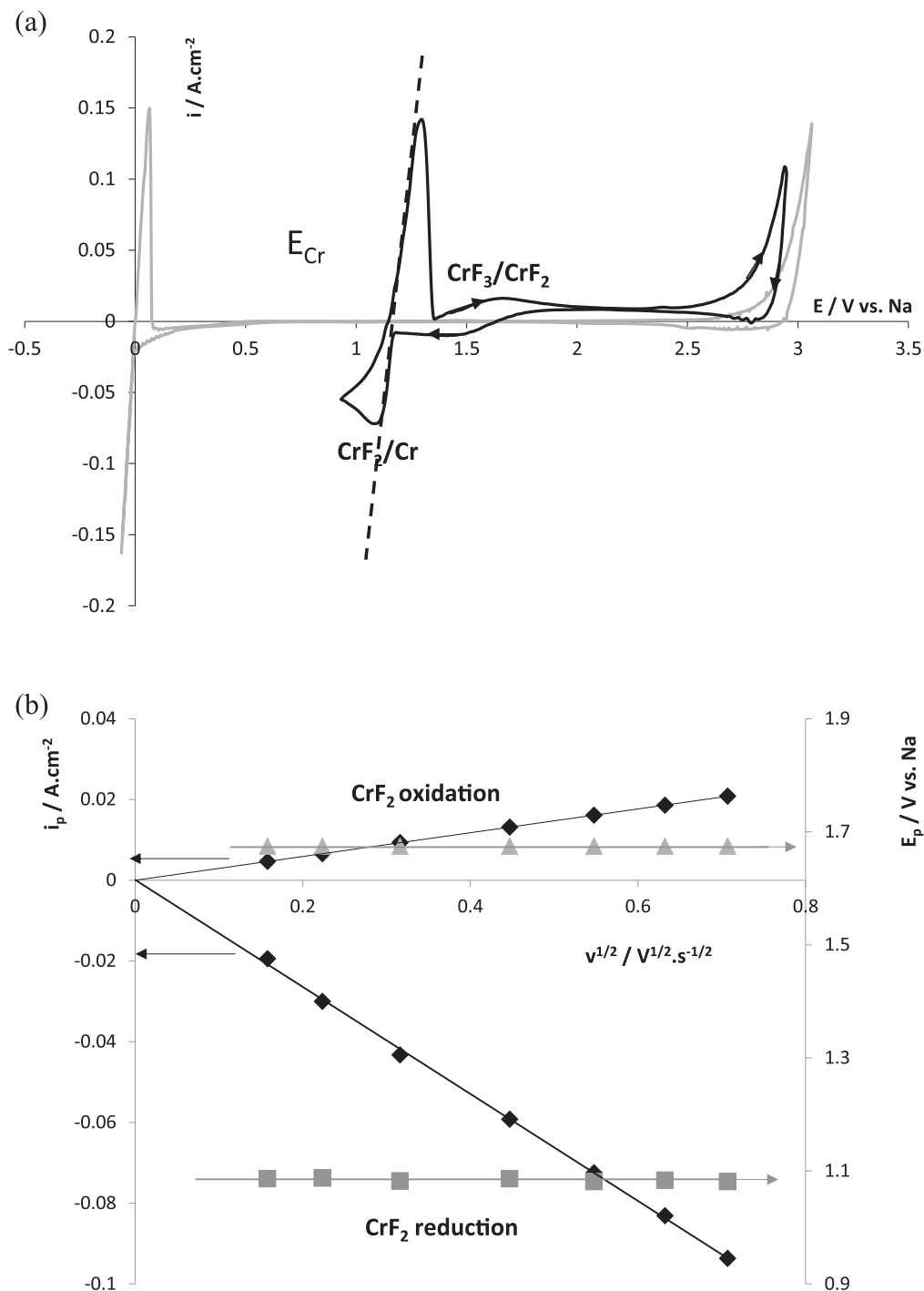


**Figure 2.** (a) Comparison of cyclic voltammograms of LiF-NaF system before (grey line) and after (black line)  $\text{CrF}_2$  addition ( $4.92 \times 10^{-2} \text{ mol kg}^{-1}$ ) on silver electrode at  $750^\circ\text{C}$  and  $100 \text{ mV s}^{-1}$ . (b) Variation of  $\text{CrF}_2$  oxidation and reduction peaks potentials and current densities vs the square root of the potential scan rate.

frequency and linear relationships are observed for both peak current densities, indicating, in agreement with cyclic voltammetry results, that  $\text{CrF}_2$  oxidation into  $\text{CrF}_3$  and  $\text{CrF}_2$  reduction into Cr are reversible and diffusion-controlled reactions.

Consequently, the number of exchanged electrons and the Cr nucleation overvoltage can be determined by measuring the half-width peak  $W_1$  for  $\text{CrF}_2$  oxidation and  $W_2$  for  $\text{CrF}_2$  reduction influenced as detailed in Ref. 10. The exchanged electrons values obtained,  $1.1 \pm 0.2$  for  $\text{CrF}_2$  oxidation and  $2.0 \pm 0.2$  for  $\text{CrF}_2$  reduction, confirming the E-pO<sub>2</sub>- diagram in Fig. 1:  $\text{CrF}_3 \leftrightarrow \text{CrF}_2 \leftrightarrow \text{Cr}$ . Using methodology

developed in our laboratory and presented in Ref. 11, the nucleation overvoltage value of Cr on silver electrode at  $750^\circ\text{C}$  was found to be  $56 \pm 4 \text{ mV}$ .

**Diffusion coefficient determination.**—Combining the results of cyclic voltammetry (Eqs. 5 and 7), the  $\text{CrF}_2$  diffusion coefficient ( $D$ ) was calculated to be  $(6.2 \pm 0.1) \times 10^{-10} \text{ m}^2 \text{ s}^{-1}$  at  $750^\circ\text{C}$ . In the  $750^\circ\text{C}$ – $900^\circ\text{C}$  temperature range, the linear variation of  $\ln D$  vs the inverse absolute temperature, plotted in Fig. 4, follows an Arrhenius' law type as:

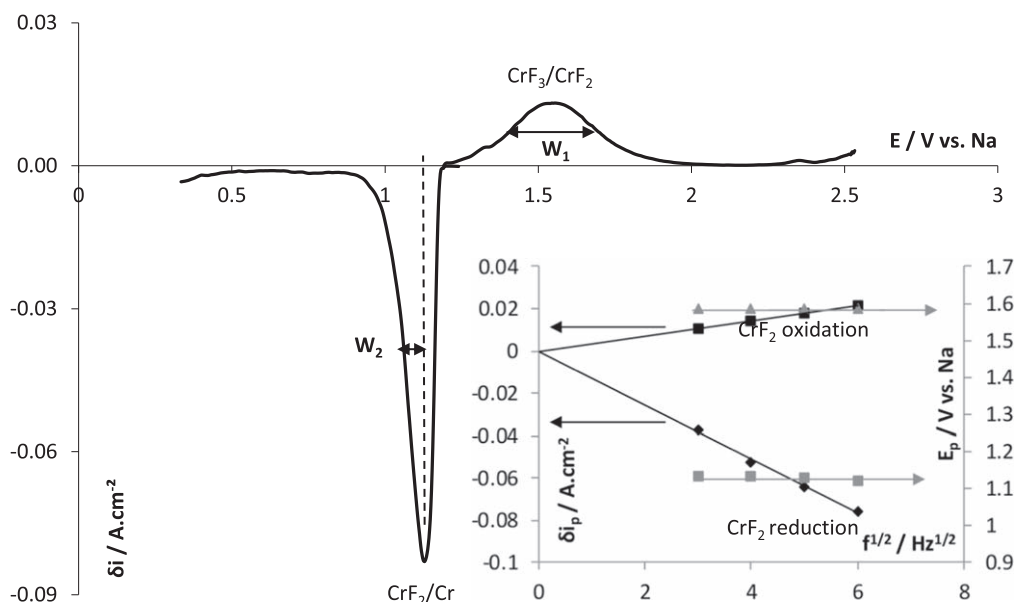


**Figure 3.** Square wave voltammograms of LiF-NaF-CrF<sub>2</sub> ( $4.92 \times 10^{-2} \text{ mol kg}^{-1}$ ) system plotted from OCP into anodic and cathodic directions on silver electrode at 750 °C and 25 Hz. Inset: Variation of CrF<sub>2</sub> oxidation and reduction peaks potentials and current densities vs the square root of the frequency.

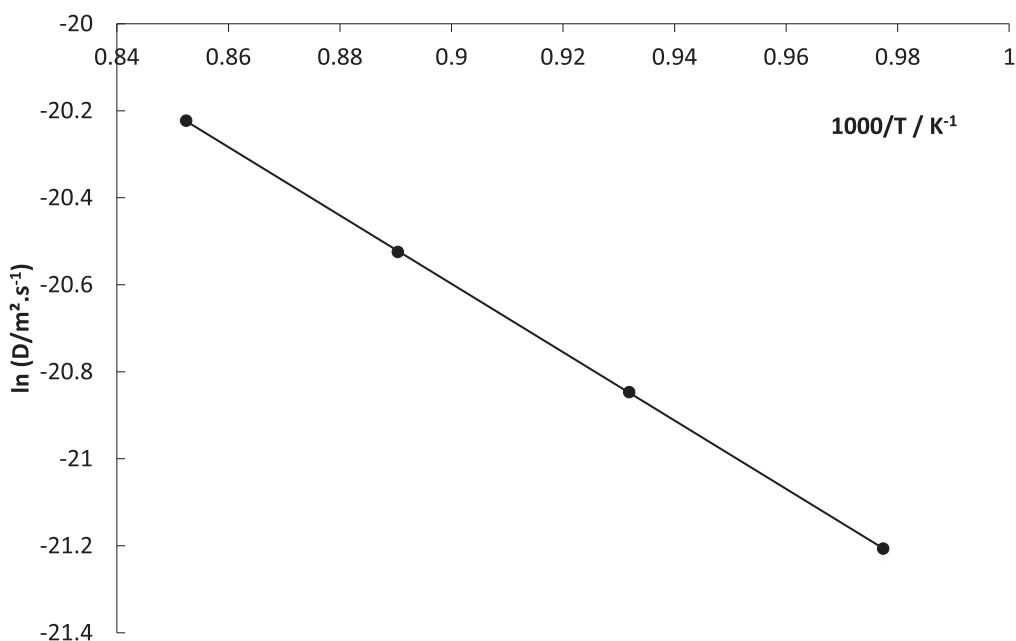


**Figure 4.** Linear relationship between the CrF<sub>2</sub> diffusion coefficient logarithm and the inverse of the absolute temperature.

$$\ln D_{(\text{m}^2\cdot\text{s}^{-1})} = -13.523 - \frac{7860.4}{T(\text{K})} \quad [10]$$

From Eq. 16, the activation energy is  $65.35 \text{ kJ mol}^{-1}$ .

This result is in good agreement with the values obtained in the bibliography for Cr(III).<sup>9,10</sup>

**CrF<sub>2</sub>/Cr standard potential and CrF<sub>2</sub> activity coefficients determination.**—CrF<sub>2</sub>/Cr standard potential.—According to the Nernst Law, the equilibrium potential of CrF<sub>2</sub>(sln)/Cr system,  $E_{\text{Cr}}$ , is expressed as follows:

$$E_{\text{Cr}} = E_{\text{CrF}_2/\text{Cr}(\text{IDRS})}^o + \frac{RT}{2F} \ln \gamma_{\text{CrF}_2(\text{sln})} + \frac{RT}{2F} \ln \frac{[\text{CrF}_2(\text{sln})]}{a_{\text{F}^{2-}}} \quad [11]$$

where  $E_{\text{CrF}_2/\text{Cr}(\text{IDRS})}^o$  is the CrF<sub>2</sub>/Cr standard potential using an infinite dilution reference state (IDRS),  $\gamma_{\text{CrF}_2(\text{sln})}$  and  $[\text{CrF}_2(\text{sln})]$  are the activity coefficient and the concentration in  $\text{mol kg}^{-1}$  of dissolved CrF<sub>2</sub> respectively.  $a_{\text{F}^-}$  is the activity of free fluoride ions in the solution.

$E_{\text{Cr}}$  can be measured from the cyclic voltammogram of LiF-NaF-CrF<sub>2</sub> system, but it must be previously converted into a reference potential scale using the F<sub>2</sub>/F<sup>-</sup> system using the equilibrium potential of NaF/Na vs F<sub>2</sub>/F<sup>-</sup>, as detailed in Ref. 12.

The change of reference potential scale can be expressed as:

$$E_{\text{Cr V vs F}_2/\text{F}^-} = E_{\text{Cr vs Na}} + E_{\text{Na vs F}_2/\text{F}^-} \quad [12]$$

where  $E_{\text{Na vs F}_2/\text{F}^-}$  was calculated using thermochemical database of HSC 6.1 software, with reference to the F<sub>2</sub>/F<sup>-</sup> system

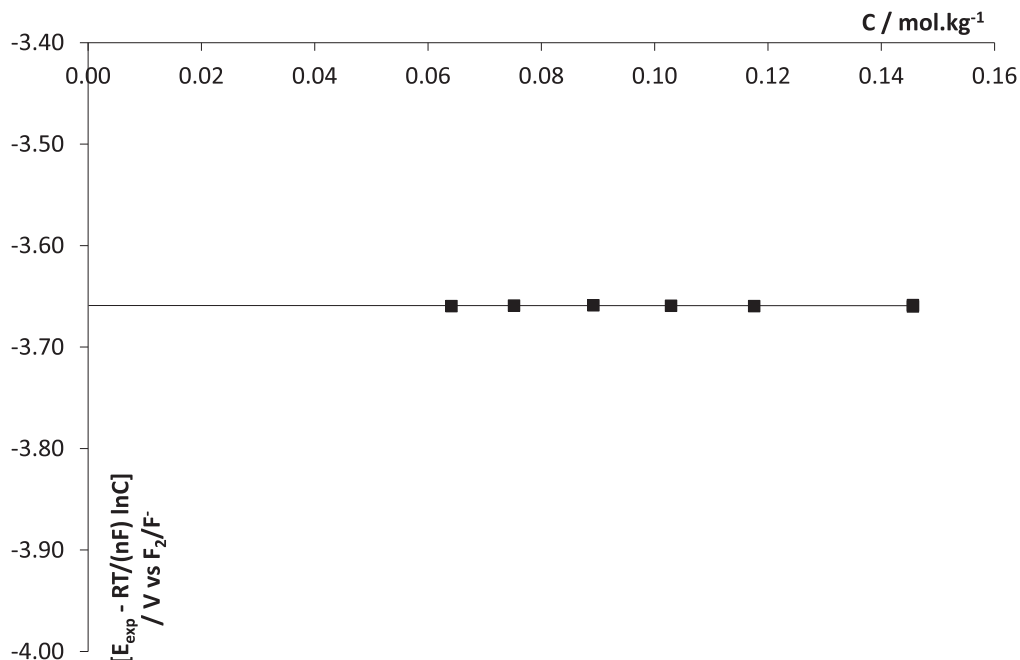


**Figure 5.** Extrapolation at infinite dilution of  $\left(E - \frac{RT}{2F} \ln [\text{CrF}_2]\right)$  vs  $[\text{CrF}_2]$ .

( $E_{\text{Na vs F}_2/\text{F}^-} = -4.95$  V) and  $E_{\text{Cr vs Na}}$  was graphically determined on the cyclic voltammogram as showed in Fig. 2a at 750 °C.

As  $E_{\text{Na vs. F}_2/\text{F}^-}$  also includes the free fluoride ions activity, the use of this difference of potential for internal reference allows to eliminate it from equations.

According to (11):

$$E_{\text{Cr}} - \frac{RT}{2F} \ln [\text{CrF}_2(\text{sln})] = E_{\text{CrF}_2/\text{Cr}}^{\circ}(\text{IDRS}) + \frac{RT}{2F} \ln \gamma_{\text{CrF}_2(\text{sln})} \quad [13]$$

So at a given temperature, it is possible to determine the  $\text{CrF}_2/\text{Cr}$  standard potential ( $E^{\circ}$ ) by extrapolating the experimental value of

$E_{\text{Cr}} - \frac{RT}{2F} \ln [\text{CrF}_2(\text{sln})]$  vs  $[\text{CrF}_2(\text{sln})]$  when

$[\text{CrF}_2(\text{sln})]$  tends towards 0; indeed, at infinite dilution  $\gamma = 1$  (see Fig. 5).<sup>11</sup>

The results of Fig. 5 allow the determination of  $\text{CrF}_2/\text{Cr}$  standard potential at 750 °C, and the obtained value is  $E_{\text{CrF}_2/\text{Cr}}^{\circ}(\text{IDRS}) = -3.65$  V vs  $\text{F}_2/\text{F}^-$ .

This value can be compared to the one obtained from Gibbs energy of pure compounds reference state (PCRS)  $\text{CrF}_2$ ,  $\Delta_f G^{\circ}$ , calculated from thermochemical database (software HSC Chemistry 6.1):

$$E_{\text{CrF}_2/\text{Cr}}^{\circ}(\text{PCRS}) = -3.35 \text{ V vs F}_2/\text{F}^-$$

The difference between the standard potentials at infinite dilution reference state and pure compound reference state represents the free energy of the dissolution and solvation reaction of  $\text{CrF}_2$  in the fluoride solution to form  $[\text{CrF}_6]^{3-}$  as mentioned by Yoko<sup>6</sup> and Nam:<sup>13</sup>



The free energy of reaction (20),  $\Delta_t G^{\circ}$ , is called transfer energy and the obtained value at 750 °C is:

$$\begin{aligned} \Delta_t G^{\circ} &= -2 F(E_{\text{CrF}_2/\text{Cr}}^{\circ}(\text{PCRS}) - E_{\text{CrF}_2/\text{Cr}}^{\circ}(\text{IDRS})) \\ &= -57 \text{ kJ mol}^{-1} \end{aligned} \quad [15]$$

**$\text{CrF}_2$  activity coefficient.**—In order to examine the ideality of  $\text{LiF-NaF-CrF}_2$  solutions using NERNST law,  $E_{\text{Cr}}$  values were

plotted vs  $\ln[\text{CrF}_2]$ , in Fig. 6. A linear relationship can be observed and the experimental slope determined is 0.044. This value is equal to the theoretical slope of Nernst law  $\left(\frac{RT}{2F}\right)$  at 750 °C, proving that  $\text{CrF}_2$  solutions are ideal up to 0.113 mol  $\text{kg}^{-1}$ .

To confirm this observation  $\text{CrF}_2$  activity coefficient ( $\gamma_{\text{CrF}_2}$ ) was calculated using the following equation derived from Eq. 13:

$$\gamma_{\text{CrF}_2} = \exp\left(\frac{2F}{RT}\left(E_{\text{Cr}} - \left(E_{\text{CrF}_2/\text{Cr}}^{\circ}(\text{PCRS}) + \frac{RT}{2F} \ln [\text{CrF}_2(\text{sln})]\right)\right)\right) \quad [16]$$

This calculation was performed for concentrations up to 0.113 mol  $\text{kg}^{-1}$ . The obtained results are reported in Table I. The values tend to 1, confirming that for this temperature and concentration range, the behaviour of  $\text{CrF}_2$  solutions is ideal.

**Influence of  $\text{Li}_2\text{O}$  additions.**—Figure 7 presents cyclic voltammograms plotted on a Ag electrode at 100  $\text{mV s}^{-1}$  in  $\text{LiF-NaF-CrF}_2$  after successive  $\text{Li}_2\text{O}$  additions: the Cr(II) reduction and oxidation peaks current densities decrease gradually with the oxide content.

The normalised quantity of Cr(II) ions  $\frac{n_{\text{CrF}_2}}{n_{\text{CrF}_2}^0}$  has been plotted vs

the normalised oxide ions content  $\frac{n_{\text{Li}_2\text{O}}}{n_{\text{CrF}_2}^0}$ , where  $n_{\text{CrF}_2}^0$  is the initial

quantity of Cr(II) present into the solution in mol,  $n_{\text{CrF}_2}$  the remaining quantity of Cr(II) in mol determined by cyclic voltammetry (cf. Eq. 5),  $n_{\text{Li}_2\text{O}}$  the added quantity of  $\text{O}^{2-}$  in mol.

The data, presented in Fig. 8, exhibit a linear relationship between the normalised quantity of oxide added and the normalised Cr(II) concentration remained in the solution with a slope value of  $-1$ . After addition of a normalized oxide content of 1.2, no more electrochemical signal related to the Cr system is observed. As reported in previous work related to rare earth,<sup>14</sup> this behaviour is an evidence of the formation of solid or non-electroactive compound.

Regarding the preliminary discussion (cf. section 3.1) and Fig. 1,  $\text{CrF}_2$  disproportionation was assumed in accordance with Eq. 4.

The experimental result is in agreement with the stoichiometry of reaction (4), confirming the assumption of the disproportionation reaction at high  $\text{O}^{2-}$  content.

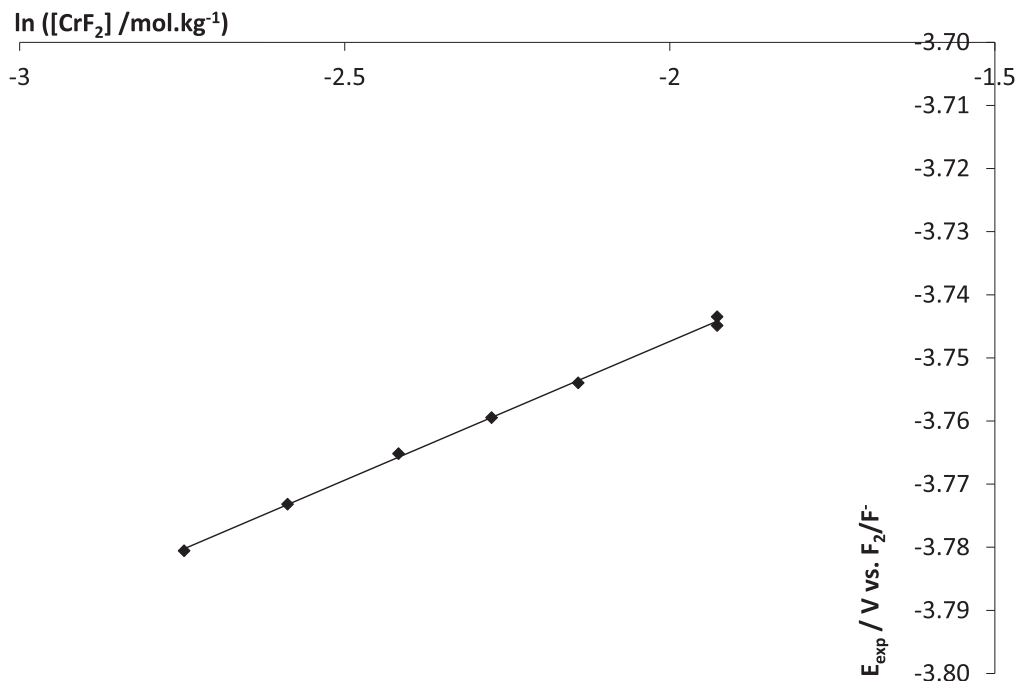


Figure 6. Variation of CrF<sub>2</sub>/Cr equilibrium potential vs the logarithm of the CrF<sub>2</sub> concentration in LiF-NaF at 750 °C.

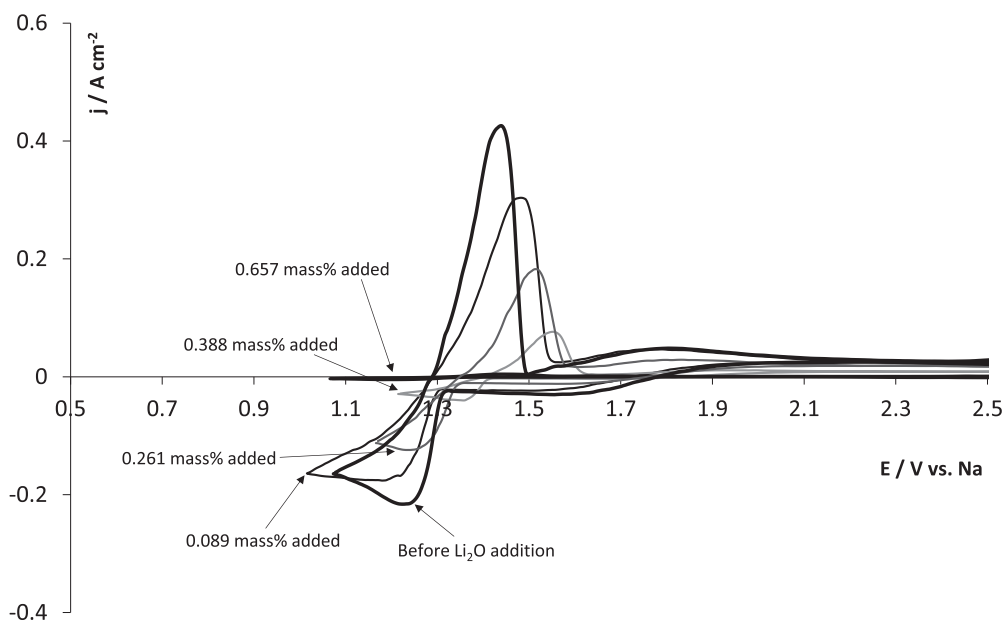


Figure 7. Superimposition of cyclic voltammograms of the LiF-NaF-CrF<sub>2</sub> system after successive Li<sub>2</sub>O additions from 0.089 mass% to 0.657 mass% on silver electrode at 750 °C and 100 mV s<sup>-1</sup>.

Table I. CrF<sub>2</sub> activity coefficient determined in the 0.050–0.113 mol kg<sup>-1</sup> range at 750 °C in LiF-NaF.

[CrF <sub>2(sln)</sub> ]/mol kg <sup>-1</sup>	0.0496	0.0581	0.0689	0.0796	0.0909	0.113
γ <sub>CrF<sub>2</sub></sub> (± 0,08)	0.99	1.00	1.01	1.00	0.99	0.99

### Conclusions

The CrF<sub>2</sub> electrochemical behaviour was investigated in LiF-NaF on silver electrode in the 750 °C–900 °C temperature range, in order to determine typical thermodynamic and physico-chemical

data. Using electrochemical techniques (cyclic and square wave voltammeteries), it was demonstrated that CrF<sub>2</sub> can be both oxidized into CrF<sub>3</sub> and reduced into Cr by diffusion-controlled reactions.

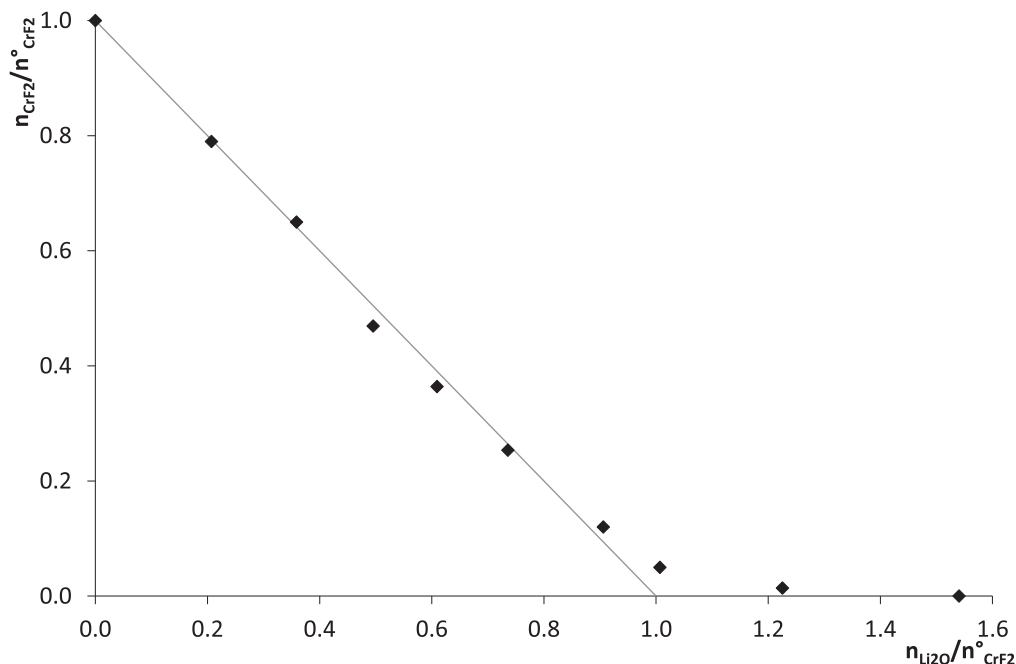


**Figure 8.** Linear relationship between added normalized quantity of  $\text{Li}_2\text{O}$  and the remaining normalized  $\text{CrF}_2$  content in the bath.

$\text{CrF}_2$  diffusion coefficients were also determined on a wide temperature range (750 °C–900 °C) and data show a dependence of  $\ln D$  with the inverse of the temperature, as a classical Arrhenius-type law.

$\text{CrF}_2/\text{Cr}$  standard potential,  $\text{CrF}_2$  activity coefficients and  $\text{CrF}_2$  transfer energy were also determined and the results showed that  $\text{CrF}_2$  solutions were ideal up to  $0.113 \text{ mol kg}^{-1}$ .

Then, the effect of oxide ions by  $\text{Li}_2\text{O}$  additions in a  $\text{LiF-NaF-CrF}_2$  system was studied at 750 °C. The chromium precipitation by  $\text{CrF}_2$  disproportionation was evidenced, as expected by analysis of thermochemical properties.

Cyclic or square wave voltammetries can be used as in situ techniques to evidence MSR materials container corrosion by  $\text{Cr(II)}$  titration into the solution.

### ORCID

L. Massot  <https://orcid.org/0000-0002-9920-2723>

### References

1. W. H. Jordan, S. J. Cromer, and A. J. Miller, *Aircraft Nuclear Propulsion Project Quarterly Progress ORNL-2387*, ORNL-2387 (1958).
2. M. W. Rosenthal, P. N. Haubenreich, and R. B. Briggs, *The development Status of Molten Salt Breeder Reactors ORNL-195*, 195 (1972).
3. W. D. Manly, D. A. Douglas, A. Taboada, and W. L. Grimes, *Fluid Fuel Reactors, Molten Salt Reactor Program—Part II. Materials studies*, ORNL-2474 (1958).
4. J. W. Koger, *Corrosion*, **29**, 115 (1973).
5. J. R. DiStefano et al., *Materials Considerations for Molten Salt Accelerator-based Plutonium Conversion Systems*, ORNL/TM-12925/R1 Oak Ridge National Laboratory (1995).
6. J. F. Smith, "The deposition of chromium from a fused fluoride electrolyte." *Thin Solid Films*, **95**, 151 (1982).
7. T. Yoko and R. A. Bailey, "Electrochemical studies of chromium in molten  $\text{LiF-NaF-KF}$  (FLINAK)." *J. Electrochem. Soc.*, **131**, 2590 (1984).
8. G. W. Mellors and S. Senderoff, *Applications of Fundamental Thermodynamics to Metallurgical Processes* (Gordon and Breach Science Publishers, New York) (1967).
9. P. Chamelot, P. Taxil, and B. Lafage, *Electrochimica Acta*, **39–17**, 2571 (1994).
10. A. J. Bard and R. L. Faulkner, *Electrochemistry: Principles, Methods and Applications* (Wiley Ed, New York) (1980).
11. C. Hamel, P. Chamelot, and P. Taxil, "Neodymium(III) cathodic processes in molten fluorides." *Electrochim. Acta*, **49**, 4467 (2004).
12. C. Nourry, L. Massot, P. Chamelot, and P. Taxil, "Data acquisition in thermodynamic and electrochemical reduction in a  $\text{Gd(III)/Gd}$  system in  $\text{LiF-CaF}_2$  media." *Electrochim. Acta*, **53**, 2650 (2008).
13. H. O. Nam, A. Bengtson, K. Vörtler, S. Saha, R. Sakidja, and D. Morgan, "First-principles molecular dynamics modeling of the molten fluoride salt with Cr solute." *J. Nucl. Mater.*, **449**, 148 (2014).
14. P. Taxil, L. Massot, C. Nourry, M. Gibilaro, P. Chamelot, and L. Cassayre, "Lanthanides extraction processes in molten fluoride media: application to nuclear spent fuel reprocessing." *J. Fluorine Chem.*, **130**, 94 (2009).